

MAGO: A NEW APPROACH FOR ORTHOPHOTOS PRODUCTION BASED ON ADAPTIVE MESH RECONSTRUCTION

S. Gagliolo, B. Federici, I. Ferrando, D. Sguerso

Università degli Studi di Genova, DICCA – Laboratory of Geodesy, Geomatics and GIS, Via Montallegro 1, 16145 Genoa, Italy
(sara.gagliolo, ilaria.ferrando)@edu.unige.it, (bianca.federici, domenico.sguerso)@unige.it

KEY WORDS: Orthophoto, Point cloud, Mesh, Images, Algorithm, Image classification, Statistical analysis

ABSTRACT:

Orthophotos are one of the most common and typical products of a photogrammetric post-processing and, since the diffusion of specific software, their generation and usage have become even more widespread. In spite of it, some issues remain on the accuracy of orthophoto reconstruction, which is often downgraded by the introduction of meshes and Digital Surface Models to be used as surfaces representing the object. The use of a more accurate and reliable input, such as a point cloud, makes these approximations avoidable. For this reason, a new approach, termed MAGO (Adaptive Mesh for Orthophoto Reconstruction), is here delineated and proposed. The input data of the procedure are the user-defined orthophoto plane, the image and its internal and external orientation parameters, and a point cloud representing the object. Each pixel of the image is projected on the orthophoto plane at its original resolution via an iterative process, which builds an adaptive mesh, defined by means of the three best fitting points, where the collinearity rays and the point cloud intersect. After an overview on the method and its innovative features, an example on a test case is reported, together with a comparison between MAGO's and another photogrammetric software results.

1. INTRODUCTION

In the last decades, the 3D survey techniques, i.e. Terrestrial Laser Scanning (TLS), Unmanned Aerial Vehicles (UAV) photogrammetry, and Light Detection and Ranging (LiDAR) acquisition, have been increasingly improved. In parallel, both the acquisition and the post-processing methods have been enhanced to obtain detailed 3D products, such as point clouds, meshes and Digital Surface Models (DSMs). Despite this, the end-users frequently request 2D products, i.e. maps, sections, and orthophotos, to ease the extraction and the interpretation of metrical information. Thus, orthophotos represent a suitable instrument to perform high-precision measurements, thanks to the uniform scale given by the orthogonal projection. For this reason, they are widely employed in several fields, mainly in cartography, but also in environmental and building engineering, cultural heritage, precision farming and forest management.

As widely known, it is possible to obtain an orthophoto starting from an image, its orientation parameters and a model of the object, typically a DSM or a mesh of the surface.

Orthophotos quality is increasing, thanks to the development of innovative techniques and technologies in the photogrammetric field. The problem of reliability in orthophotos production has given rise to the research on True Orthophotos© (Amhar, 1998; Habib et al., 2007; Wang et al., 2018), which are focused on the combination of two masked orthophotos, that represent buildings and terrain of an urban area separately, to avoid misrepresentation and lack of information in hidden areas. Based on the described criterion, some tools have been implemented to generate accurate orthophotos, e.g. TORPEDO (Three dimensional Object Resource Package for Enhancing Digital Orthophotos; Amhar, 1998), ACCORTHO (ACCurate ORTHOprojection; Boccardo et al., 2001), GCOOrtho (Geometrically Corrected Orthophotos; Barazzetti et al., 2007).

Moreover, many photogrammetric software packages, both commercial (e.g. Agisoft Metashape©, 2019; ContextCapture™, 2019; Pix4D©, 2019; LiMapper©, 2019; Orto©, 2019) and open source (MicMac, 2019;

OpenDroneMap, 2019) include a specific step for orthophotos reconstruction, typically at the end of their workflow, when the polygonal mesh is already available.

The traditional strategies provide for direct front views of the point cloud or orthophoto reconstruction starting from DSM or mesh. The present work introduces a different approach in order to limit the approximation given by the representation of the object via a point cloud discretization and, at the same time, to reach the best possible resolution.

The point cloud is used to reconstruct a step-by-step adaptive mesh of the object. To reconstruct the orthophoto, each pixel of the considered image is related to the corresponding portion of the point cloud through the collinearity equations. Then, an interpolating plane is created starting from the three best-fitting neighbouring points. The exact intersection between the collinearity ray projected by the image and the plane itself is determined and consequently orthogonally projected on the user-defined orthophoto plane.

This method, named MAGO (Adaptive Mesh for Orthophoto Generation), has been implemented in C++ environment, with the support of some existing open source tools: Cimg Library (2019), Image Magick (2019), and matrix.h (2019). Cimg Library and Image Magick have been used to operate images, also in different file formats, while matrix.h allowed an ease management and calculation of data stored in matrices.

The present dissertation is organized as follows: the MAGO approach and workflow are described in section 2; the considered case study is presented in section 3; MAGO preliminary results are presented in section 4, together with a comparison with the results of another software and some statistical analyses.

The conclusions are reported in the last section.

2. MAGO APPROACH AND WORKFLOW

As already stated, the 3D products are typically transformed into 2D ones to ease their management and interpretation. Generally, the following strategies are available:

1. front views of the point cloud, according to a defined point of view;
2. traditional orthophoto realized starting from a previously computed DSM;
3. orthophoto realized by photogrammetric software with embedded mesh and orthophoto reconstruction phases.

In cases 1 and 2, the highest resolution of the 2D product is in the order of the point cloud mean spacing; in case 3, the highest resolution is comparable with the Ground Sample Distance (GSD) size, but the object description is depleted due to a simplified approach to realize the polygons of the mesh.

In this context, the MAGO software has been developed to avoid this rough simplification by means of a step-by-step adaptive mesh from the point cloud. Moreover, it allows to reconstruct the highest possible resolution orthophoto, in the same order of the GSD of the original image.

The MAGO approach for orthophoto generation is designed to consider a specific triangular plane area where the image pixel is projected at its original resolution, avoiding the approximation and loss of definition typically introduced by the mesh reconstruction phase.

The MAGO workflow consists in the following phases, which will be described in the following sections:

1. definition of the orthophoto plane;
2. acquisition of internal and external orientation parameters and images themselves from external sources;
3. definition of the orthophoto dimensions and resolution;
4. iterative process to determine the three best-fitting points, that define the plane where the collinearity ray and the point cloud intersect;
5. the corresponding colour of each pixel in the image is projected on the orthophoto plane.

Points 1-3, termed *preliminary input and settings*, are described in section 2.1, while the iterative process, which is the core of MAGO procedure, is described in section 2.2.

On sakes of simplicity, the procedure is here delineated for a single image, even if MAGO is able to process multiple images.

2.1 Preliminary input and settings

Firstly, the point cloud representing the object, produced by external photogrammetric software processing or acquired by TLS or LiDAR, has to be uploaded in MAGO. It is suggested to provide a filtered input point cloud because MAGO is not yet able to filter autonomously.

The internal and external orientation (IO and EO) parameters of the image must be previously obtained using an external software and are given as an input, together with the image itself.

The user is then requested to define the orthophoto plane, via the coordinates of three points, expressed in either a local or an external reference system with projected coordinates.

The orthophoto resolution is user-defined, and it should be adequately chosen considering the GSD of the image, in order to get an optimal final result.

The orthophoto dimensions are automatically computed by MAGO considering the point cloud's minimum and maximum values along each dimension. In this way, the highest possible orthophoto dimensions are:

$$\frac{X_{MAX} - X_{MIN}}{\text{resolution}} = \text{orthophoto width}$$

$$\frac{Y_{MAX} - Y_{MIN}}{\text{resolution}} = \text{orthophoto height} \quad (1)$$

The orthophoto boundaries can also be user-defined, for example in case the orthophoto should represent only a detail of the entire object, but obviously the limits in Equation (1) remain valid.

A regular grid, with resolution in the order of the point cloud spacing, is then created to store the original positions and related additional information (e.g. RGB fields, intensity, normal components, etc.) of the input points, in order to be able to easily recover the whole point cloud information avoiding a memory overload. The data contained in the grid will be used in the following step for the orthophoto generation. Moreover, they can eventually be used to generate a DSM of the object by using several pre-set criteria, such as mean, median, and maximum value of points heights in each cell.

Finally, the user could set a downscaling factor for the original image in order to speed up the procedure and to match the orthophoto resolution.

All these settings can be inserted via a Graphical User Interface (GUI), as depicted in Figure 1.

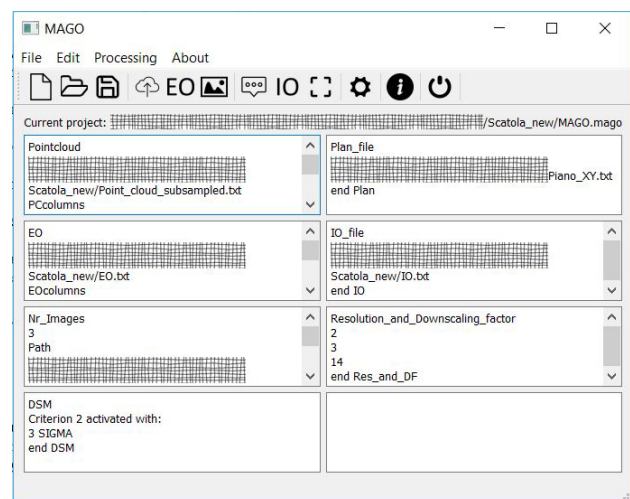


Figure 1. MAGO's Graphical User Interface.

Once the input parameters have been defined, the processing for orthophoto generation could start.

2.2 Iterative process for orthophoto generation

The orthophoto is obtained by means of an iterative process to determine the plane where the collinearity ray from each pixel and the point cloud intersect. This plane is one of the faces of the adaptive mesh which approximates the point cloud describing the object. Each face of the adaptive mesh is generated directly from the input point cloud, without any further simplification, re-sampling or approximation of the point cloud itself, thus the adaptive mesh is the highest-resolution mesh possible.

To build the orthophoto, the procedure starts from the collinearity equations applied on each pixel on the image.

$$x = x_0 - c \frac{r_{11}(X_P - X_0) + r_{12}(Y_P - Y_0) + r_{13}(Z_P - Z_0)}{r_{31}(X_P - X_0) + r_{32}(Y_P - Y_0) + r_{33}(Z_P - Z_0)}$$

$$y = y_0 - c \frac{r_{21}(X_P - X_0) + r_{22}(Y_P - Y_0) + r_{23}(Z_P - Z_0)}{r_{31}(X_P - X_0) + r_{32}(Y_P - Y_0) + r_{33}(Z_P - Z_0)} \quad (2)$$

Among the parameters reported in Equation (2), the image coordinates (x, y) , the IO parameters (focal length c , and principal point coordinates, x_0, y_0), and the EO parameters (camera positions $\underline{X}_0 = (X_0, Y_0, Z_0)$ and r_{ij} components of the

Cardano rotation matrix \mathbf{R} are known; on the contrary, the point coordinates $\underline{X}_p = (X_p, Y_p, Z_p)$ are unknowns.

At the beginning of the iterative process, the first attempt Z_p is imposed equal to Z_{MAX} , which represents the maximum height of the points in the point cloud, having preferably excluded and filtered out the outliers. X_p and Y_p are consequently computed, applying the collinearity equations.

The so-obtained \underline{X}_p coordinates match a cell of the grid (defined in the preliminary phase of the procedure) and its corresponding pixel on the orthophoto plane.

Considering the candidate cell of the grid, the correspondence is confirmed if there is a point falling inside the volume defined by the cell dimensions and a threshold along z , termed δz and fixed on the basis of the point cloud spacing s .

In this case, two possible scenarios are considered, based on the distance between the found point and the collinearity ray. If they are less distant than a threshold given by the GSD size affected by the downscaling factor, the point itself is considered as a correspondence between the image and the orthophoto pixel, and it is projected on the orthophoto plane. In case the threshold is exceeded, the algorithm searches in the cell itself and in its 8 neighbours the two other points, to build a triangle with the first one.

The chosen criteria to define the best-fitting triangle are delineated in the following. Due to the point cloud inhomogeneity, the points that are too near or too far from the first found one have to be excluded to avoid an unrealistic description of the surface.

A threshold is defined as a ring with internal (r_i) and external (r_e) radius respectively of 40% and 180% of the cloud spacing.

To avoid the definition of a sub-vertical plane, a cylinder is introduced as follows: the base is the previously defined ring, while the height (h) ranges within a distance proportional to the external diameter of the ring and the tangent of $\pm 80^\circ$. Moreover, at least one of the two candidate points has to be on the opposite side of the track of collinearity ray on the orthophoto plane, with respect to the first one. Finally, the found vertices have to respect a minimum projected area of the triangle equal to 20% of the regular grid cell area. Thus, the intersection between the adaptive triangle, defined by these three best fitting points, and the collinearity ray determines the final correspondence between the image pixel and the orthophoto one.

The chosen criteria and thresholds are depicted in Figure 2.

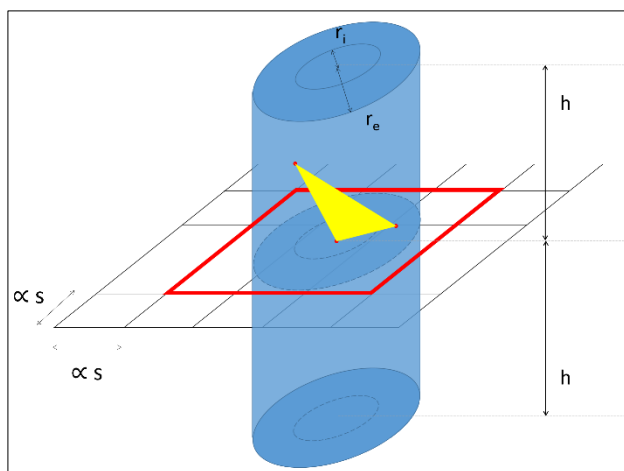


Figure 2. Criteria and parameters of adaptive meshing and matching iterative process.

In case the threshold δz is not complied or the cell is empty, Z_p is automatically decreased of the spacing s and the updated Z_p

value is used for the iterative process, until a correspondence is found. If the value of Z_{MIN} (representing the minimum height of the points in the point cloud) is reached without having found a matching, the pixel is discarded and the procedure continues with the analysis of a new one, until all the pixels on the image have been analysed.

Figure 3 depicts the scheme of MAGO workflow.

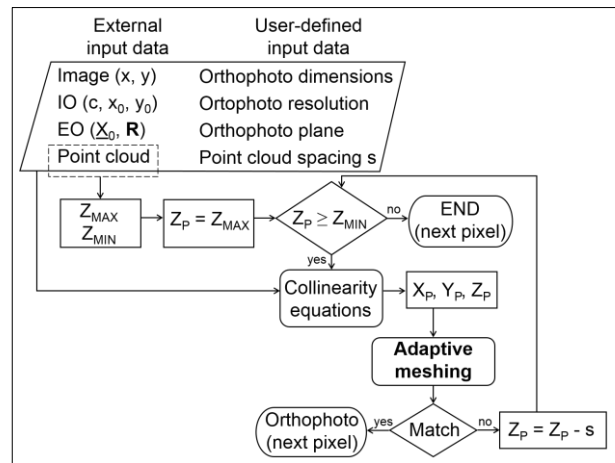


Figure 3. MAGO workflow.

3. APPLICATION TO A CASE STUDY

The whole procedure has been tested on a simple laboratory case study using a box over a checkerboard. Three nadiral images have been acquired with a Canon EOS 40D camera with a focal length of 22 mm, at a distance of about 1.10 m. The resulting GSD is 0.3 mm. The images have been processed using Agisoft Metashape®, i.e. Agisoft PhotoScan® renewed version, and the resulting dense cloud has been filtered from noise using CloudCompare (2019). The final point cloud has about 4500 points, with a mean point spacing of 10 mm. The so-obtained point cloud has been directly processed with MAGO, while it has been imported in Agisoft Metashape® and substituted to the dense cloud for the meshing and the orthophoto reconstruction. This guarantees the coherence of the input data in the two methods of orthophoto generation.

The grid cell dimension s is fixed to a precautionary value of 14 mm, to be almost sure to find at least one point in the cell and to minimize the empty cells.

IO and EO have been exported from Agisoft Metashape® processing. The central image has been chosen for the orthophoto reconstruction, which is realized over the horizontal (XY) plane.

The resolution of the orthophoto has been set to 2 mm, so the theoretical downscaling factor results lower than 7, taking into account the ratio between the orthophoto resolution and the original GSD, as in the following equation:

$$\text{downscaling factor} = \frac{\text{orthophoto resolution}}{\text{original GSD}} = \frac{2}{0.3} < 7 \quad (3)$$

As a precaution, the final downscaling factor has been fixed to 3 in order to avoid a loss of resolution in the input image and, consequently, in the orthophoto. Thus, the image downscaled GSD results $0.3 \times 3 = 0.9$ mm, that is significantly lower than the orthophoto pixel size.

The boundaries have been automatically acquired from the limits of the point cloud, which represents a portion of the whole scene, as depicted in Figure 4.

Finally, the local reference system has its origin in the bottom-left vertex of the left checkerboard, and it is oriented as follows:

1. X axis along the bottom side, oriented to the right;
2. Y axis along the left side, oriented to the top;
3. Z axis orthogonal to the floor, oriented upward.

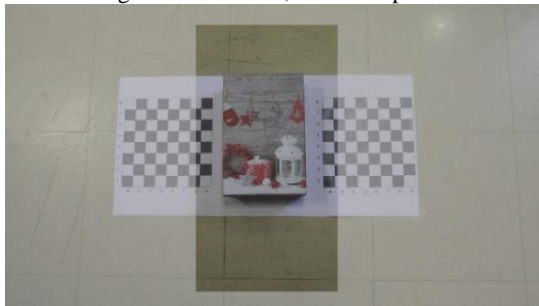


Figure 4. Analyzed portion for orthophoto reconstruction.

4. RESULTS AND DISCUSSION

As already mentioned, the most common existing photogrammetric software provide for orthophoto generation at a certain step of their workflow, typically after the generation of a mesh or a DSM from the point cloud. On the contrary, MAGO employs the point cloud to generate the orthophoto at its highest possible resolution, exploiting the original resolution of the images, that are projected over the adaptive mesh according to the IO and EO parameters. The resulting orthophoto is represented in Figure 5a, where the black areas correspond to no-match pixels. In Figure 5b, the DSM of the input point cloud highlights that the holes in Figure 5a correspond to empty cells, due to border effects and to lack of data around the box.

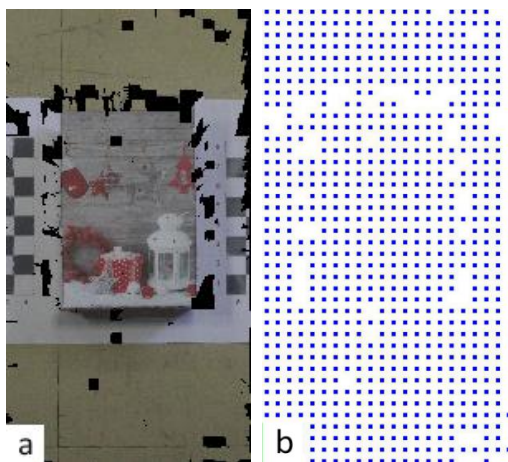


Figure 5. Orthophoto (a) and DSM (b) generated by MAGO.

The orthophoto derived from MAGO and Agisoft Metashape© using the same settings, i.e. orthophoto plane, pixel size, orthophoto boundaries, processed image and input point cloud, are compared in the following.

The processing of the latter software has been set using the “Height field” surface type (which is the most suitable for planar objects, as the present case is) and the medium “Face count” for the mesh reconstruction, using the input filtered point cloud as input. The interpolation has been disabled, in order to reconstruct the mesh only where points are present. Then, the textured model has been realized, specifying to use only the central image and disabling the hole filling.

Considering the available options to build the orthophoto in Agisoft Metashape©, the pixel size is customizable. A default

value, assumed as the highest theoretical value, is suggested according to the average GSD of the original images. Then, the dimensions of the orthophoto are automatically computed, based on the pixel and the mesh dimensions.

The orthophoto projection plane is chosen by means of three points (*markers*, representative of Ground Control Points, GCP), or defining a plane parallel to pre-defined views or to a user-defined current view.

The user may also choose the limits of the orthophoto by operating on the boundary settings, in case only a specific portion of the mesh should be represented in the orthophoto.

The orthophotos derived from MAGO and Agisoft Metashape© are depicted in Figure 6, where the black areas represent holes in the orthophoto reconstruction.

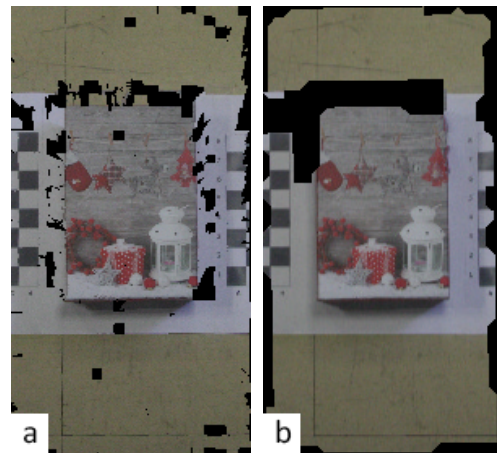


Figure 6. Orthophoto generated by MAGO (a) and by Agisoft Metashape© (b).

Figure 6 underlines similarities and differences in the outputs: both of them present holes around the box; MAGO produces more scattered and sparser no-data areas, whereas Agisoft Metashape© concentrates them around the box and along the image boundaries. Moreover, MAGO orthophoto seems clearer, with sharper transitions in colors between adjacent pixels.

In Figure 7, the orthophotos have been analysed in order to classify the holes generated only by MAGO (yellow), only by Agisoft Metashape© (cyan), and by both software (magenta). The background orthophoto is the one generated by MAGO.



Figure 7. Comparison between holes in the orthophotos produced by MAGO and Agisoft Metashape©: yellow, cyan and magenta represent the holes produced by only MAGO, only Agisoft Metashape©, and both, respectively.

Moreover, in Table 1 the number of cells and the percentage cover with respect to the orthophoto size ($148 \times 277 = 40996$ cells) are reported. The number of no-data cells is obtained as follows: the yellow and cyan are the total hole cells produced by MAGO and Agisoft Metashape© respectively, having already removed the common ones (magenta).

The computation of the intersection area, the related statistics and the following elaborations have been performed using GRASS GIS 7.4 (2019).

Orthophoto holes	Cell count	Percentage cover
MAGO only (yellow)	1563	3.81%
Agisoft Metashape© only (cyan)	4720	11.51%
Both (magenta)	1817	4.43%

Table 1. Comparison between MAGO and Agisoft Metashape© orthophoto holes: cell count and percentage cover data.

Another statistical analysis has been performed on the three bands (Red, Green and Blue; hereafter R, G, B) of the two orthophotos. Considering each band separately, the previously individuated holes areas have been removed, assigning a no-data value. Then, the difference between MAGO and Agisoft Metashape© has been computed via a raster algebra calculator, obtaining values in the range of about -100 to +100. The three differences maps have been classified according to the following ranges:

- class 1: difference values in the interval [-100;-20];
- class 2: difference values in the interval [-20;20];
- class 3: difference values in the interval (20;100].

The result of the classification is depicted in Figure 8 (a, b and c refer to R, G, and B bands respectively), where the grey areas correspond to class 2, whereas blue and red pixels lie into class 1 and 3, respectively.

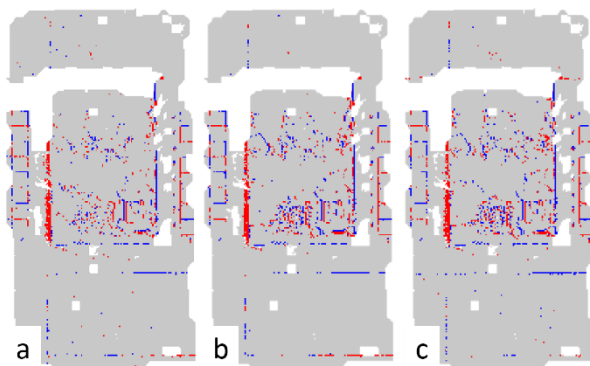


Figure 8. Classification of difference maps (MAGO-Agisoft Metashape©) for R (a), G (b), and B (c) bands. Class 1, 2 and 3 are represented in blue, grey and red, respectively

Observing Figure 8, it is evident that the difference between the two orthophoto is limited between -20 and +20 for the majority of pixels (the ones represented in grey color). The most marked differences are located along the borders of the box and the checkerboard and, in general, where a sharp change of color in adjacent pixels is present, e.g. along the outlines of the floor tiles and of the squares on the checkerboard. Moreover, a more scattered pattern of high differences can be noticed over the box

cover; again, it can be imputable to the change of color between neighbouring pixels.

Table 2 summarizes the number of cells and the percentage cover of each class for the difference map, with analogous values for the three bands.

It should be noted that the total number of cells is 32743 for each band (instead of $148 \times 277 = 40996$), because the pixels corresponding to holes have been previously removed. The percentage covers are computed accordingly; indeed, the sum of percentage cover for each band is 100%.

	Class	Cell count	Percentage cover
Red band	1	536	1.64%
	2	31469	96.11%
	3	738	2.25%
Green band	1	633	1.93%
	2	31238	95.41%
	3	872	2.66%
Blue band	1	674	2.06%
	2	31209	95.32%
	3	860	2.62%

Table 2. Classification of difference maps on the RGB bands: cell count and percentage cover data for the three classes.

A final summary map of differences has been computed, as reported in Figure 9.

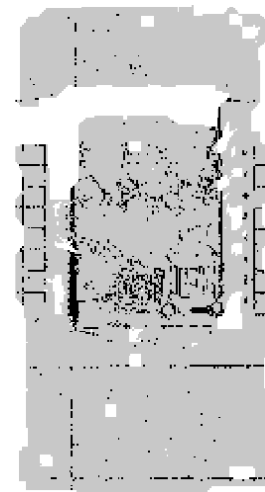


Figure 9. Summary of difference maps for the three bands. The grey and black pixels respectively represent areas of agreement and disagreement between the bands of the two orthophotos.

The grey pixels represent the areas where the R, G and B bands present a difference value between MAGO and Agisoft Metashape© within class 2, i.e. limited in the range of -20 and +20, whereas the black pixels correspond to areas where the considered pixel lies in class 1 or 3 for at least one of the three bands. Summarizing, the grey pixels can be interpreted as areas of limited differences for the three bands, namely areas where the two orthophotos are quite similar. Conversely, the black pixels highlight a disagreement of the different bands of the two orthophotos, and they will be object of future investigations.

5. CONCLUSIONS AND FUTURE PERSPECTIVES

In the present work, a new method for orthophoto reconstruction, termed MAGO (Adaptive Mesh for Orthophoto Reconstruction) is introduced. The proposed approach allows to obtain orthophotos at high resolution, comparable with the image Ground Sample Distance (GSD), using as input a reliable point cloud. Each pixel of the image is projected on the orthophoto plane at its original resolution via an iterative process, which builds an adaptive mesh, defined by means of the three best fitting points, where the collinearity rays and the point cloud intersect. Thus, it is possible to overcome the issues related to resolution (typical of both front views and DSM-derived orthophoto) and approximation due to the a priori polygonal mesh reconstruction.

MAGO has been used to produce an orthophoto of a simple laboratory test case, consisting in a box over a checkerboard, starting from a photogrammetric point cloud, properly filtered from noise. The same point cloud has been used as input for Agisoft Metashape© workflow for orthophoto generation, which involves the mesh reconstruction as first step.

The presented results and the comparison with the orthophoto generated using Agisoft Metashape© show that, as expected, the most critical areas for orthophoto reconstruction are located along the borders of the box, where the point cloud is incomplete due to the sub-vertical planes generated by the box sides. In those areas, both MAGO and Agisoft Metashape© can not reconstruct the mesh: MAGO avoids the pixel filling where it is not able to build the adaptive mesh, due to an insufficient number of input points, whereas Agisoft Metashape© has been run with the interpolation and hole filling options disabled. This produces holes in both the orthophotos, which have been statistically analyzed in terms of number of involved pixels and percentage of cover. Moreover, they have been classified according to the software from which they have been generated (only MAGO, only Agisoft Metashape©, or both). The difference maps have been also computed between each band of MAGO and Agisoft Metashape© orthophotos and a classification has been performed to analyze the similarity between the two orthophotos also from the color bands point of view.

The future perspectives will focus on the orthophoto isolated holes filling, the point cloud filtering through the regular grid per-cell statistics, and the orthomosaic generation. Generating an orthomosaic will also improve the completeness thanks to the integration of multiple orthophotos, also considering True Orthophoto© theoretical principles in order to establish the final matching.

Furthermore, the possibility to choose the orientation of the orthophoto plane will be improved, using the Rodrigues' formulation to rotate both the point cloud and the EO parameters in the rotated reference system.

Lastly, several tests will be carried out to optimize the parameters settings and to evaluate the MAGO performances.

REFERENCES

Amhar F., Jansa J., Ries C., 1998. The generation of true orthophotos using a 3D building model in conjunction with a conventional DTM. *International Archives of Photogrammetry and Remote Sensing*, 32(4), pp. 16-22

Barazzetti L., Brovelli M., Scaioni M., 2007. Problems Related to the Generation of True-Orthophotos with LiDAR DDSMs. In: *Proc. ISPRS Work. "Laser Scanning 2007 and SilviLaser 2007"*, Espoo (Finland), 12-14 Sept, The International Archives

of the Photogrammetry, Remote Sensing and Spatial Information Sciences, Vol. XXXVI, Part 3/W52, pp. 20- 26
Boccardo P., Dequal S., Lingua A., Rinaudo F., 2001. True Digital Orthophoto for architectural and archaeological applications. *The International Archives of the Photogrammetry, Remote Sensing and Spatial Information Sciences*, Vol. XXXIV-5/W1, 2001. *International Workshop on Recreating the Past-Visualization and Animation of Cultural Heritage*, 26 February – 1 March 2001, Ayutthaya, Thailand

Habib A. F., Kim E., Kim C., 2007. New Methodologies for True Orthophoto Generation. *Photogrammetric Engineering & Remote Sensing*, Vol. 73, No. 1, January 2007, pp. 025–036

Wang Q., Yan L., Sun Y., Cui X., Mortimer H., Li Y., 2018. True orthophoto generation using line segment matches. *The Photogrammetric Record*, 33(161), pp. 113-130. DOI: 10.1111/phor.12229. 2018

Agisoft Metashape©, 2019, <http://www.agisoft.com/> (access on 5th March 2019)

CloudCompare, 2019, <http://www.cloudcompare.org/> (access on 5th March 2019)

ContextCapture™, 2019, <https://www.bentley.com/it> (access on 5th March 2019)

GRASS GIS, 2019, <https://grass.osgeo.org/> (access on 5th March 2019)

MicMac, 2019, <http://micmac.ensg.eu/> (access on 5th March 2019)

OpenDroneMap, 2019, <http://opendronemap.org/> (access on 5th March 2019)

Pix4D, 2019, <https://pix4d.com/> (access on 5th March 2019)

VisualSFM, 2019, <http://ccwu.me/vsfm/> (access on 5th March 2019)

Z+F LaserControl®, 2019, <https://www.zf-laser.com/> (access on 5th March 2019)